J|A|C|S
ARTICLES

Published on Web 01/09/2009

Polymer Nanoparticles: Shape-Directed Monomer-to-Particle Synthesis

Tao He,[†] Dave J. Adams,[†] Michael F. Butler,[‡] Andrew I. Cooper,*[,†] and Steve P. Rannard*[,†]

Department of Chemistry and Centre for Materials Discovery, University of Liverpool, Crown Street, Liverpool, L69 7ZD, U.K., and Unilever Corporate Research, Colworth, Sharnbrook, Bedfordshire, MK44 1LQ, U.K.

Received September 19, 2008; E-mail: aicooper@liv.ac.uk; srannard@liv.ac.uk

Abstract: Well-defined dumbbell and tripartite organic nanoparticles (30−60 nm) were produced *via* a one-pot direct synthesis of branched amphiphilic block copolymers, avoiding the need for postsynthesis self-assembly steps. We show the mechanism of dumbbell formation is largely a concerted process of particle growth during polymerization, although data suggest that particle−particle linking also occurs, particularly at higher monomer conversions. Dumbbell particles formed using a disulfide bifunctional initiator lead to cleavable structures, underlining the role of initiator functionality in shape control and the potential for functionality placement. Trifunctional initiators allow the direct one-pot synthesis of "tripartite" clover-leaf shaped nanoparticles which would be difficult to achieve through conventional synthesis/self-assembly/cross-linking strategies.

Introduction

The direct synthetic control of organic nanoparticle shape using covalent bond-forming reactions represents a significant synthetic challenge. There are very few examples of the direct synthesis of complex, nonspherical particulate organic materials. Instead, strategies to postorganize nanoparticles into ordered architectures have generally been pursued.[1]

Several strategies have been employed to produce spherical organic nanoparticles including solution and emulsion syntheses, for example, dendrimers,[2] branched vinyl free-radical polymerization,[3] emulsion polymerization,[4] mini-emulsion polymerization[5] and emulsion/evaporation techniques.[6] Due to the complexities of direct monomer-to-nanoparticle syntheses, indirect assembly strategies utilizing amphiphilic block copolymers have been widely reported, with optional cross-linking of the self-assembled structures. For example, polymer-based vesicles,[7] polymer-caged small-molecule liposomes,[8] phase-separated self-assembled block copolymers,[9] and shell-cross-linked micelles[10,11] have been produced by such strategies. Surface energy minimization during self-assembly can lead to a variety of structures,[12] but spherical particles dominate these reports. Control of nanoparticle shape has been demonstrated using new lithographic techniques[13] and micron-sized dumbbells have been generated by phase-separation during the polymerization of monomer swollen polymer particles,[14] but neither of these examples represent a direct shape-directed covalent synthesis.

We recently reported the direct monomer-to-particle synthesis of amphiphilic spherical and dumbbell polymer nanoparticles[15] utilizing a combination of controlled atom transfer radical polymerization (ATRP) techniques[16,17] and branched vinyl polymerization.[18,19] Our strategy differs significantly from arm-first or core-first core-cross-linked star-polymer synthesis where the core is effectively a highly cross-linked microgel formed by the addition of a high concentration of a cross-linker such

[†] University of Liverpool.
[‡] Unilever Corporate Research.

(1) Yao, H.; Yi, C.; Tzang, C. H.; Zhu, J.; Yang, M. *Nanotechnology* **2007**, *18*, 015102/1–015102/7.
(2) (a) Lee, C. C.; MacKay, J. A.; Fréchet, J. M. J.; Szoka, F. C. *Nat. Biotechnol.* **2005**, *23*, 1517–1526. (b) Tomalia, D. A.; Fréchet, J. M. J. *Prog. Polym. Sci.* **2005**, *30*, 217–219. (c) Fréchet, J. M. J. *J. Polym. Sci. A1* **2003**, *41*, 3713–3725. (d) Grayson, S. M.; Fréchet, J. M. J. *Chem. Rev.* **2001**, *101*, 3819–3867. (e) Aulenta, F.; Hayes, W.; Rannard, S. *Eur. Polym. J.* **2003**, *39*, 1741–1771.
(3) Weaver, J. V. M.; Williams, R. T.; Royles, B. J. L.; Findlay, P. H.; Cooper, A. I.; Rannard, S. P. *Soft Matter* **2008**, *4*, 985–992.
(4) Pecher, J.; Mecking, S. *Macromolecules* **2007**, *40*, 7733–7735.
(5) Musyanovych, A.; Schmitz-Wienke, J.; Mailaender, V.; Walther, P.; Landfester, K. *Macromol. Biosci.* **2008**, *8*, 127–139.
(6) Babak, V. G.; Baros, F.; Boulanouar, O.; Boury, F.; Fromm, M.; Kildeeva, N. R.; Ubrich, N.; Maincent, P. *Colloids Surf. B* **2007**, *59*, 194–207.
(7) Li, B.; Martin, A. L.; Gillies, E. R. *Chem. Commun.* **2007**, 5217–5219.
(8) Lee, S.-M.; Chen, H.; Dettmer, C. M.; O'Halloran, T. V.; Nguyen, S. T. *J. Am. Chem. Soc.* **2007**, *129*, 15096–15097.
(9) Hales, K.; Chen, Z.; Wooley, K. L.; Pochan, D. J. *Nano Lett.* **2008**, *8*, 2023–2026.
(10) Butun, V.; Billingham, N. C.; Armes, S. P. *J. Am. Chem. Soc.* **1998**, *120*, 12135–12136.
(11) Read, E. S.; Armes, S. P. *Chem. Commun.* **2007**, 3021–3035.
(12) Stupp, S. I.; LeBonheur, V.; Walker, K.; Li, L. S.; Huggins, K. E.; Keser, M.; Amstutz, A. *Science* **1997**, *276*, 384–389.
(13) Rolland, J. P.; Maynor, B. W.; Euliss, L. E.; Exner, A. E.; Denison, G. M.; DeSimone, J. M. *J. Am. Chem. Soc.* **2005**, *127*, 10096–10100.
(14) Kim, J.-W.; Larsen, R. J.; Weitz, D. A. *J. Am. Chem. Soc.* **2006**, *128*, 14374–14377.
(15) He, T.; Adams, D. J.; Butler, M. F.; Yeoh, C. T.; Cooper, A. I.; Rannard, S. P. *Angew. Chem. Intl. Ed.* **2007**, *46*, 9243–9247.
(16) Wang, J. S.; Matyjaszewski, K. *J. Am. Chem. Soc.* **1995**, *117*, 5614–5615.
(17) Matyjaszewski, K.; Xia, J. *Chem. Rev.* **2001**, *101*, 2921–2990.
(18) Bannister, I.; Billingham, N. C.; Armes, S. P.; Rannard, S. P.; Findlay, P. *Macromolecules* **2006**, *39*, 7483–7492.

Scheme 1. Schematic Representation of Synthetic Strategy Producing (A) Spherical Polymer Nanoparticles with a Poly(OEGMA)-stabilized Poly(*n*BuMA) Core and (b) Dumbbell Polymer Nanoparticles Showing Two Poly(OEGMA)-stabilized Poly(*n*BuMA) Cores Covalently Connected by a Bifunctional Poly(OEGMA) Chain Derived from Initiator **2**[a]

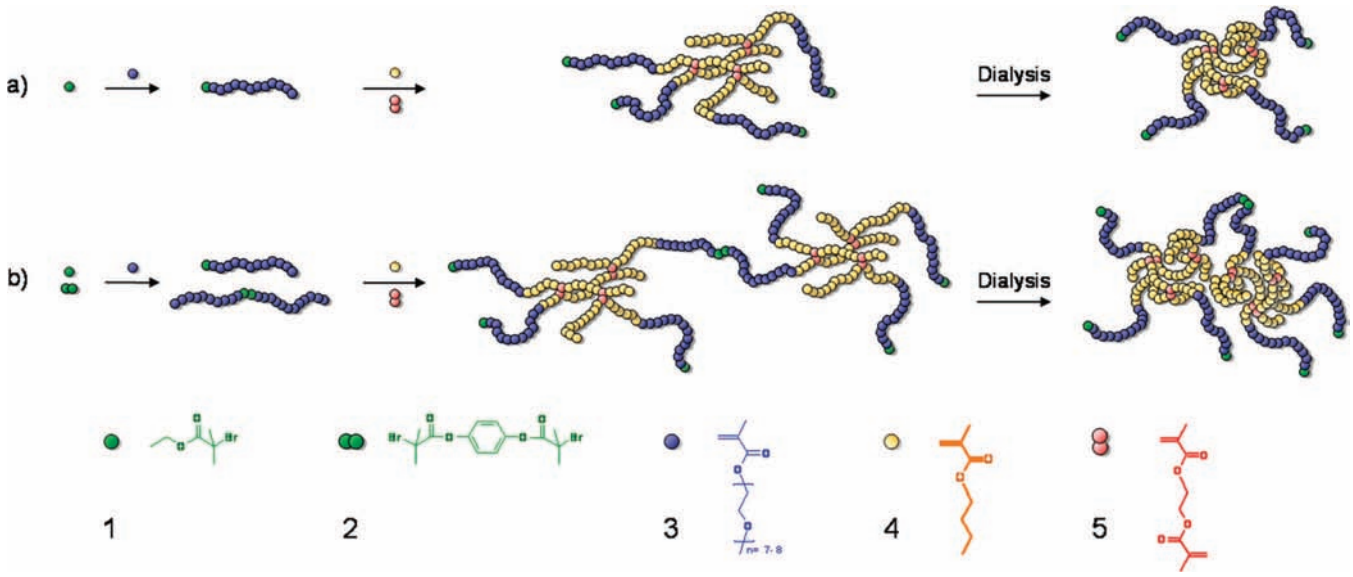

[a] In both cases, dialysis from THF to water results in collapse of poly(*n*BuMA) branched cores.

as divinylbenzene.[20−28] In contrast to these approaches, we rely upon the confinement of branches to the hydrophobic second block copolymer segment of a one-pot A-B branched block copolymerization conducted under waterborne ATRP conditions,[29] and branching is restricted to be, on stoichiometric average, less than one branch per A-B block copolymer chain. After the initial synthesis of a hydrophilic block copolymer segment, addition of a mixed second monomer feed, consisting of a monovinyl monomer (*n*-butyl methacrylate, *n*BuMA) and a small amount of divinyl monomer (ethylene glycol dimethacrylate, EGDMA, less than 2% of the molar ratio for the core) forms a branched hydrophobic core. Branch points are incorporated statistically during growth of the second block segment, and covalent bonding between many chains occurs via a concerted propagation/branching process during core formation. After dialysis to remove solvent, the branched hydrophobic core segments collapse but are prevented from precipitating by stabilization imparted by the hydrophilic block segments.

Using this strategy, we showed that it is possible to prepare amphiphilic materials which adopt defined spherical structures in solution, highly reminiscent of block copolymer micelles. The addition of bifunctional ATRP initiators allowed the formation of anisotropic dumbbell particles.[15] Here, we report further insights into the mechanism by which these spherical and dumbbell nanoparticles are generated and demonstrate that this simple one-pot, controlled free-radical branching polymerization can be extended to prepare "tripartite", shaped polymer nanoparticles without requiring self-assembly and/or subsequent cross-linking steps. Crucially, we show that the shape of the particles is directed by the initiator geometry.

Results and Discussion

We have previously demonstrated the synthesis of spherical and dumbbell particles via a controlled branching strategy[15] using conventional ATRP initiators, **1** and **2** (Scheme 1). The sequential polymerization strategy generates an initial hydrophilic block segment (poly(oligo(ethyleneglycol) methacrylate), pOEGMA, **3**) followed by the copolymerization of a mixed hydrophobic monomer feed containing vinyl (*n*BuMA, **4**) and divinyl (EGDMA, **5**) monomers. The ratio of the EGDMA brancher to initiator is controlled to be less than 1:1, and as such, the growing hydrophobic blocks are able to branch and form bonds with other growing chains. This results in covalently linked A-B block copolymer chains without the formation of a macromolecular network and macrogelation. Discrete spherical polymer nanoparticles are formed at high solid loadings when using a monofunctional initiator **1**. This strategy was extended to produce dumbbell particles via the inclusion of a bifunctional initiator, **2**, which generates a small number of A-B-A block copolymer bridging chains and leads to asymmetric nanoparticle synthesis (Scheme 1).[15]

The synthesis of spherical nanoparticles is intuitively straightforward, but the mechanism involved in generating dumbbells is less obvious. Solvent effects leading to anisotropy via phase separation have been discounted as the mixed isopropanol/water (92.5/7.5% v/v) solvent system has been previously shown to aid the ATRP polymerization of *n*BuMA to form linear homopolymers,[29] single and dumbbell particles are formed using identical solvents, and the branched copolymerization of *n*BuMA/EGDMA under these conditions shows controlled ATRP

(19) (a) O'Brien, N.; McKee, A.; Sherrington, D. C.; Slark, A. T.; Titterton, A. *Polymer* **2000**, *41*, 6027–6031. (b) Graham, S.; Rannard, S. P.; Cormack, P. A. G.; Sherrington, D. C. *J. Mater. Chem.* **2007**, *17*, 545–552.
(20) Gao, H.; Matyjaszewski, K. *Macromolecules* **2006**, *39*, 3154–3160.
(21) Gao, H.; Matyjaszewski, K. *J. Am. Chem. Soc.* **2007**, *129*, 11828–11834.
(22) Du, J.; Chen, Y. *J. Polym. Sci., Part A: Polym. Chem.* **2004**, *42*, 2263–2271.
(23) Zheng, Q.; Zheng, G.; Pan, C. *Polym. Int.* **2006**, *55*, 1114–1123.
(24) Baek, K.; Kamigaito, M.; Sawamoto, M. *Macromolecules* **2002**, *35*, 1493–1498.
(25) Baek, K.; Kamigaito, M.; Sawamoto, M. *Macromolecules* **2001**, *34*, 7629–7635.
(26) Gao, H.; Matyjaszewski, K. *Macromolecules* **2008**, *41*, 1118–1125.
(27) Ishizu, K.; Katsuhara, H.; Itoya, K. *J. Polym. Sci., Part A: Polym. Chem.* **2006**, *44*, 3321–3327.
(28) Terashima, T.; Ouchi, M.; Ando, T.; Kamigaito, M.; Sawamoto, M. *Macromolecules* **2007**, *40*, 3581–3588.
(29) McDonald, S.; Rannard, S. P. *Macromolecules* **2001**, *34*, 8600–8602.

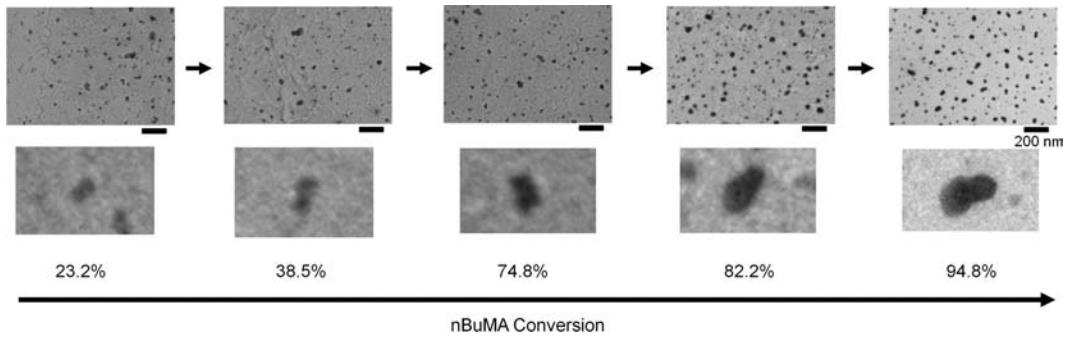

Figure 1. Observation of nascent dumbbell particles during the branched block copolymerization at various conversions of the second block derived from *n*BuMA. In all cases, the scale bar represents 200 nm.

kinetics (see Supporting Information, SI). In principle, there are two nonexclusive mechanisms by which the dumbbell nanoparticles could form: (a) coupling of preformed spheres and (b) concerted growth directed by the presence of the bifunctional initiator. Sampling during the branched *n*BuMA/EGDMA polymerization of the second block segment, using a mixture of initiators **1** and **2**, followed by dialysis and transmission electron microscopy (TEM), allowed direct observation of the structures being formed during the generation of the hydrophobic core. A *concerted growth mechanism* is implied by the presence of nascent dumbbell structures (<20 nm in length) at relatively low *n*BuMA conversions (<25% conversion), as depicted in Figure 1. The nascent dumbbells were not representative of all structures observed by TEM, and many spherical particles were also observed leading to a relatively high particle size distribution at these low monomer conversions. It is also difficult to make definitive judgements for the entire sample at these low monomer conversions since TEM suggests significant agglomeration of these nascent species on the TEM grid. Particle uniformity and the proportion of dumbbells increased significantly with *n*BuMA conversion during the particle growth process (Figure 1; see SI, Figure S3 and S4). A similar increase in particle uniformity was also observed during the synthesis of spherical nanoparticles produced in the absence of **2** (see SI, Figure S1 and S2). In both cases, larger (>100 nm) amorphous species were also seen at very low monomer conversions (<20%), probably associated with lower molar mass film-forming material.

The general behavior observed for both spherical particle and dumbbell particles systems is consistent with previous kinetic investigations of the ATRP branched copolymerization of 2-hydroxypropyl methacrylate and EGDMA.[18] In that study, it was shown that the reaction of EGDMA is statistical, following near ideal behavior with no competitive reaction compared to the monovinyl monomer; however branching and the formation of very high molecular weight species occur in the latter stages of the polymerization. These species are formed as the "free" or lightly branched polymer chains are consumed, therefore driving the uniformity of the particle distribution at high conversions. Since the proportion of dumbbell structures increases with *n*BuMA conversion, which is related to EGDMA consumption, it is also likely that some particle−particle coupling plays a role at higher monomer conversions, in addition to "concerted" growth at lower conversions. In principle, the coupling of particles does not require the presence of a bifunctional initiator and dumbbells may theoretically be produced *via* the reaction of the growing chain ends of one particle core reacting with pendant vinyl groups present on another particle. Dumbbell structures were never observed, however, for the reactions carried out in the absence of **2**, suggesting that this does not occur under these reaction conditions.

To investigate further the role of initiator **2** during dumbbell formation, we prepared an analogous bifunctional initiator, bis[2-(2-bromoisobutyryloxy)ethyl] disulfide, **6**, which contains a cleavable disulfide bridge.[30] In the absence of a branching molecule, initiator **6** was shown to generate low dispersity linear ABA block copolymers under standard ATRP conditions using sequential block copolymerization of **3** and **4** (see SI), thus behaving in a manner similar to that of **2**. The disulfide bridge present within the linear ABA block copolymers could be successfully cleaved, following the literature procedure with dithiothreitol (DTT, **7**),[31] to form linear AB block copolymers with approximately half of the number average molecular weight of the initial ABA macromolecule (see SI).

Incorporation of a mixture of **1** and **6** (monofunctional/bifunctional initator ratio **1/6** = 80:20) into a two-step sequential one-pot branched copolymerisation of OEGMA and *n*BuMA/EGDMA (Scheme 2, OEGMA/*n*BuMA = 40:60) again resulted in a preponderance of dumbbell structures (Figure 2A and 2C). Both the ratio of dumbbell structures with respect to spherical structures (51% by number) and the average size of the dumbbell structures (mean length = 56 nm as measured by TEM) were very similar to those reported previously for the equivalent noncleavable bifunctional initiator, **2**.[15] These particles were dissolved in THF, and the disulfide bridges within the initiator residues of **6** were cleaved with DTT (Scheme 2).

Dynamic light scattering (DLS) analysis of the polymer nanoparticle dispersions before and after cleavage indicated very similar particle sizes with a z-average diameter of 33 nm before cleavage and 31 nm after cleavage. It should be noted here that DLS analysis assumes a spherical geometry, whereas a large proportion of the particles before cleavage are anisotropic, and as such, this comparison should be considered as qualitative only. There was a significant decrease in the polydispersity index from 0.126 before cleavage (presence of spherical and dumbbell structures) to 0.074 after cleavage (almost exclusively spherical structures), indicative of an increase in the uniformity of the system postcleavage and the loss of the larger dumbbell structures within the precleavage distribution. TEM imaging after dialysis clearly demonstrated that the proportion of dumbbell structures was greatly reduced postcleavage (Figure 2B) from 51% to just 1.1% dumbbells by number (>900 particles counted, Figure 2C).

(30) Tsarevsky, N. V.; Matyjaszewski, K. *Macromolecules* **2005**, *38*, 3087–3090.
(31) Tsarevsky, N. V.; Matyjaszewski, K. *Macromolecules* **2002**, *35*, 9009–9014.

Scheme 2. Schematic Representation of the Synthesis and Cleavage of Dumbbell Particles Using a Mixed Monofunctional/Disulfide Bifunctional Initiator System

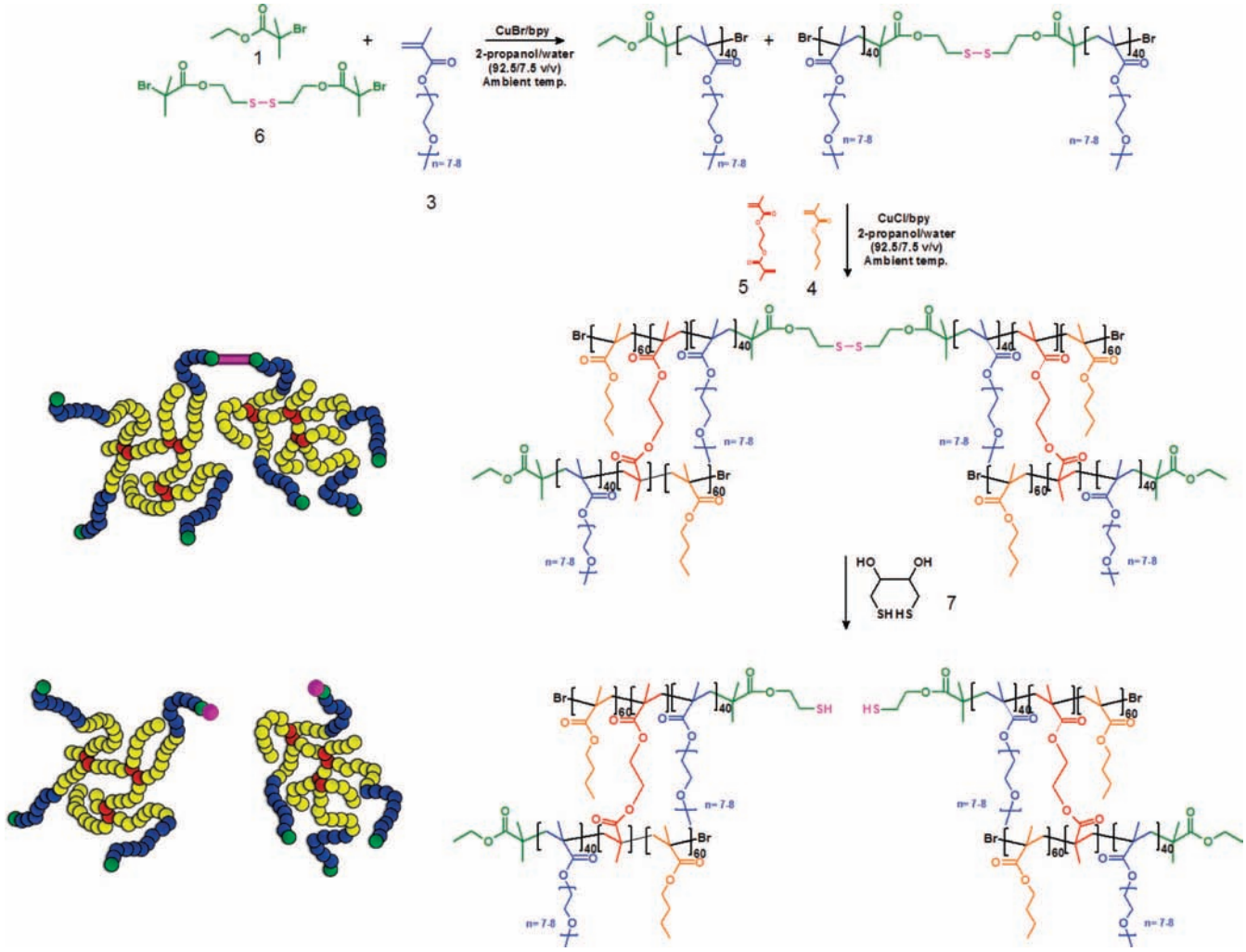

These data demonstrate unambiguously that the dumbbell nanoparticles are linked almost exclusively *via* the bifunctional initiated ABA triblock copolymer chains rather than by interparticle core−core branching *via* EGDMA residues. Structures produced through this latter process would not be cleaved by the DTT reaction. The data also support a predominantly concerted growth mechanism directed by the bifunctional initiator, although particle−particle coupling and structure buildup *via* capture of a second nascent core by a bifunctionally initiated polymer "arm" at higher conversions cannot be ruled out. To gain further insight into the nanoparticle growth, we exposed the single particles after cleavage to a solution of 2 nm gold nanoparticles (GNPs) stabilized with butanethiol.[32] The material was subjected to extensive dialysis (7000 Da cutoff) to remove unbound GNPs. Control experiments involving spherical polymer nanoparticles or uncleaved dumbbell particles showed no binding of gold to the polymer; that is, clear, colorless solutions were observed after dialysis, indicating complete removal of the gold (Figure 3). Likewise, TEM images of these control polymers after dialysis and deposition on a TEM gird showed no evidence for gold nanoparticle attachment to the nanoparticles (see SI). In contrast, significant GNP attachment was observed for the spherical nanoparticles formed *via* dumbbell cleavage, presumably through interaction with the thiol residues at the particle surface. These materials formed stable "solutions" which remained colored even after extensive dialysis. TEM images showed clearly the presence of GNPs associated with the cleaved polymer nanoparticles (Figure 3, right). A number of the cleaved polymer nanoparticles contained several bound GNPs (>10 GNPs per polymer nanoparticle), suggesting multiple thiol functionalities. We cannot be sure, however, that each GNP binds to just a single thiol residue. Moreover, there may be thiol functionality that is "buried" within the polymer nanoparticle core and hence unable to react with gold. Nevertheless, these data do strongly suggest that each polymer dumbbell contains more than one bifunctionally initiated chain and probably at least 10 such chains per dumbbell entity. Given the likely molar masses of the dumbbells ($\sim 10^7$ g/mol),[15] this is expected on a purely statistical basis and it is likely that a number of arms would contribute to dumbbell formation; that is, multiple bifunctional initiators are consumed in each dumbbell thereby increasing the probability of single particle formation. We cannot be sure that every cleaved arm contributed to core−core branching and dumbbell formation, but it is nonetheless remarkable that more than 50% of the particles formed were dumbbell-shaped and very few higher-order structures were

(32) Brust, M.; Walker, M.; Bethell, D.; Schiffrin, D. J.; Whyman, R. J. *Chem. Commun.* **1994**, 801–802.

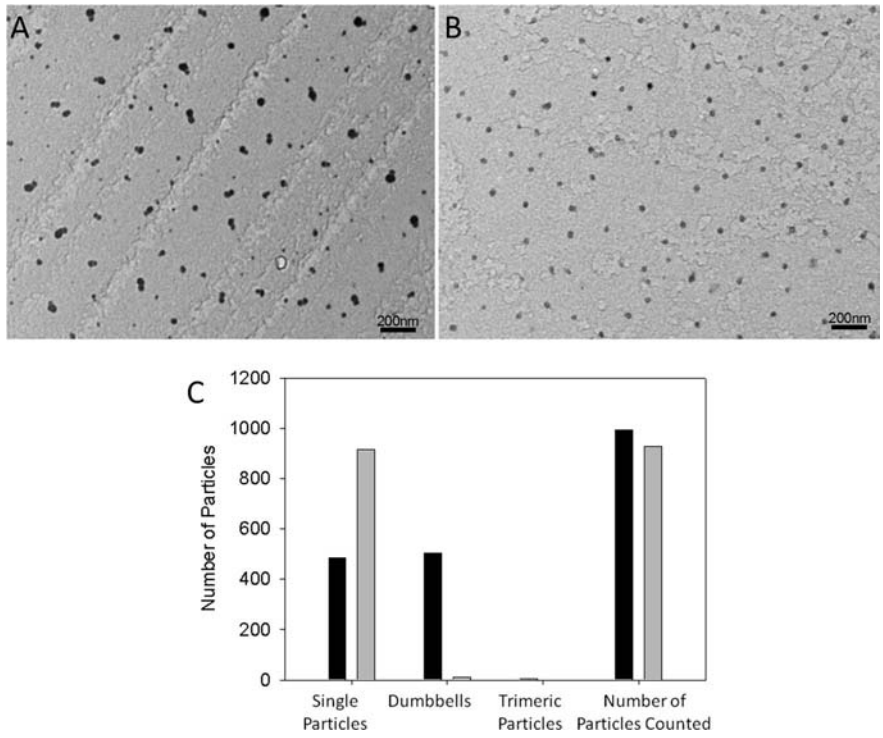

Figure 2. Evaluation of dumbbell particle shape before and after bifunctional initiator cleavage. (A) TEM image of dumbbell nanoparticles formed using a cleavable bifunctional initiator. (B) TEM image of dumbbell sample after cleavage, showing spherical particles. (C) Particle distributions before (black) and after (gray) cleavage.

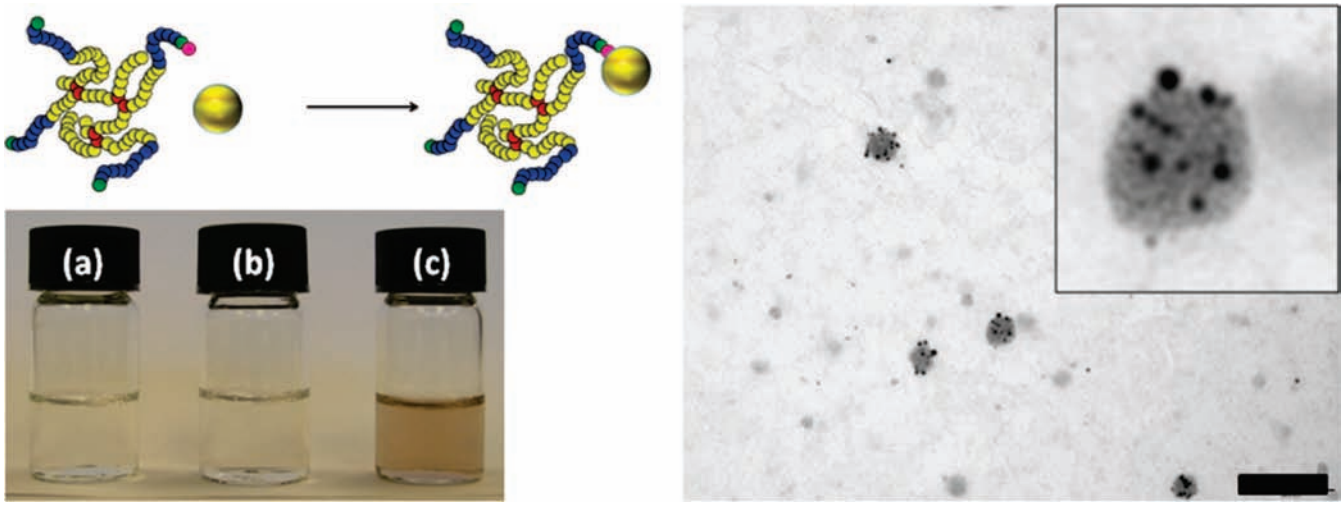

Figure 3. (Top Left) Schematic showing binding of gold nanoparticle to branched polymer with exposed thiol group. (Bottom left) Solutions of (a) spherical nanoparticles prepared using a monofunctional initiator[15] (b) dumbbell particles before cleavage and (c) dumbbell particles after cleavage exposed to gold nanoparticles followed by extensive dialysis. (Right) TEM showing dumbbell particles after cleavage exposed to gold nanoparticles followed by extensive dialysis with insert showing expansion of one of the particles. The scale bar represents 200 nm.

formed, given that these data suggest that there are a sufficient number of such bifunctional polymer arms to allow "stringing together" of particles. As speculated previously,[15] it is probable that some bifunctionally initiated chains do not participate in core−core bridging, forming "intracore" loops and "dangling" chains which do not contribute to this linking process.[15] Given the soft nature of these polymer nanoparticles, we believe that it is not possible to infer detailed structural information from the spatial distribution of the GNPs around the polymer nanoparticle core. It seems improbable that a "patch" of gold-decorated thiol functionality would be observed at the remains of a cleaved dumbbell interface since (i) significant structural reorganization is expected to occur after cleavage and during the dialysis protocol and (ii) thiol functionality will exist from initiator residues that did not participate in dumbbell formation prior to cleavage.

As demonstrated using mixed initiators **1** and **2**,[15] and subsequently confirmed using **1** and **6**, an 80:20 ratio of monofunctional to bifunctional initiator may also lead to a small number of higher order nanostructures being formed in addition to the spherical and dumbbell structures discussed above. This is expected in a statistically governed reaction. For example, both linear and triangular "three-core" or "trimeric" structures were evident in TEM images from mixed initiator systems.

Scheme 3. Schematic Representation of Initiator-Directed "Tripartite" Nanoparticle Synthesis Directed by the Trifunctional Initiator

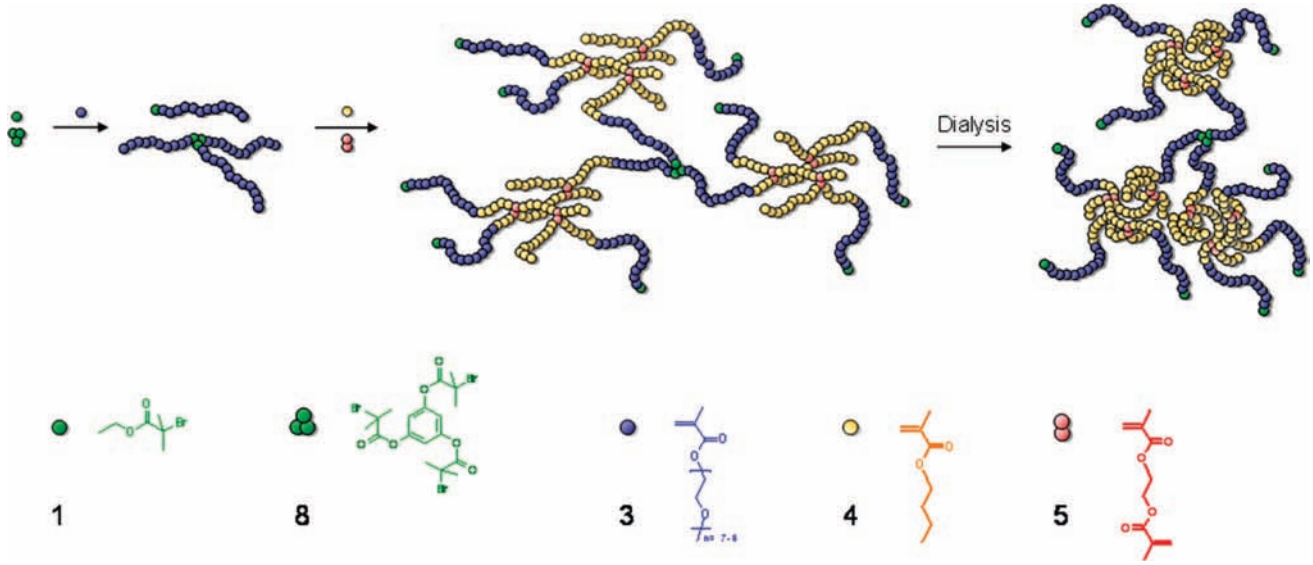

These structures were also cleaved by treatment with DTT when employing initiator **6**, Figure 2C. Attempts to form an increased population of well-defined higher order structures by further manipulating the monofunctional to bifunctional initiator ratio were unsuccessful and resulted in macroscopic network formation and gelation.[15] We therefore speculated that a mixed mono/*trifunctional* initiation system could produce initiator-directed "tripartite" nanostructures with three cores arranged in defined shapes (Scheme 3) rather than our previous two-core dumbbells and uncontrolled higher order structures described above.

A trifunctional initiator, **8**, was synthesized *via* the reaction of 1,3,5-trihydroxybenzene with 2-bromoisobutyryl bromide (see SI). **8** was shown to generate narrow dispersity three-armed star block copolymers under standard ATRP conditions using sequential block copolymerization of **3** and **4** (see SI). To form branched nanoparticles, a mixture of trifunctional and monofunctional initiators, **8** and **1**, was used to polymerize 60 units of **3** per bromide initiation site, followed by addition of a mixed monomer feed comprising **4** and **5** (66.6:1 ratio) using synthesis conditions similar to those reported previously.[16,22] This equates to an overall **5**/Br ratio of 0.9:1, thereby ensuring branching rather than cross-linking in the second stage of polymerization. After purification, the polymers were dissolved in THF and dialyzed for at least 2 days to give clear, stable nanodispersions (see SI) which were analyzed by TEM and DLS (see SI).

At a 15:85 ratio of **8/1** (60:60 ratio of **3/4**), we observed a mixture of nanoparticle morphologies (Z-average diameter (DLS) = 39 nm). TEM analysis (Figure 4D) showed the sample consisted of single spherical particles (65% by number of 580 particles sampled), similar to those observed for monofunctional initiating systems in our previous study,[15] combined with "tripartite" particles (31% by number). A very small population of two-core "dumbbells" was also observed in the sample (2.8% by number). As before, the average particle sizes measured by TEM were larger than those measured by DLS,[15] indicating a degree of collapse and spreading on the TEM grid. These specific tripartite structures were *not* observed in our previous study[15] other than as rare trimeric occurrences (<0.5% of species by number). Moreover, previous higher-order species exhibited a broad range of morphologies (e.g., linear "strings" of three cores, triangular-type assemblies), whereas the variable-sized tripartite structures here almost all exhibited a broadly triangular "club" or "clover leaf" structure (Figure 4D). Analysis of TEM images of particles produced by polymerizations containing monofunctional, mixed mono/bifunctional, and mixed mono/trifunctional initiators shows a clear trend toward control of particle shape directed by initiator functionality and geometry (Figure 4A−C). When using a monofunctional initiator alone, only spherical particles are observed (Figure 4A, >900 particles sampled; 40:60 ratio of **3/4**). When a mono/bifunctional mixed initiator system was used (Figure 4B), a large percentage (56%) of two-core "dumbbells" are formed (>900 particles sampled; 40:60 ratio of **3/4**) and <0.5% of species have more than two cores.[15] The introduction of a mono/trifunctional initiator mixture directs the production of tripartite structures (Figure 4C) almost to the exclusion of other higher-order particles and, within the limits of our current analysis methods, intriguingly, to the near exclusion of two-core "dumbbells" (histogram, Figure 4C). It should be noted that these number average distributions (spherical versus dumbbells versus tripartite) significantly overestimate the *weight* percentage of the lower mass spherical particles.

Increased connectivity between joined cores with increased initiator functionality can be rationalized by simple statistical linking behavior. However, particle−particle "capture" during growth might be expected to give a more statistical average distribution of species and structures. The very small number of dumbbell structures for the trifunctional initiator case (Figure 4C) and the sharp asymmetry of the distribution for the bifunctional system (56% dumbbells, <0.5% higher order species) both suggest a more direct transfer of initiator geometry to the final particle. This is surprising, given the soft nature of these solids and also because it is very probable (by statistics and by analogy with the GNP-labeling study discussed above) that each polymer nanoparticle incorporates many more than one trifunctionally initiated chain, as opposed to the very simplistic representations given in Schemes 1, 2 and 3. Thus, the degree of core−core linking observed does not reflect the potential of the system to form more extended structures such as long chains of particle cores. One possible reason for this is that a proportion of bi- and trifunctionally initiated chains are inactive in terms of core−core linking as a result of loop formation and other side reactions. Again, this does not imply that the cores are linked by single bifunctional or trifunctional

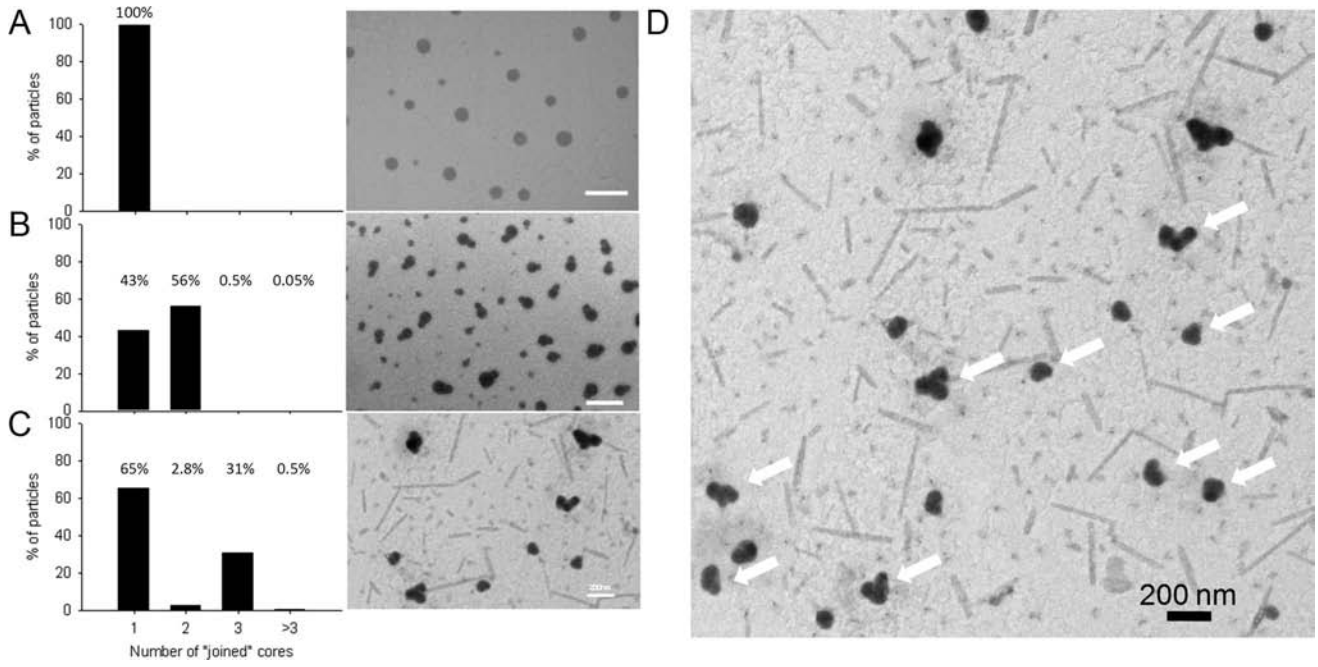

Figure 4. TEM analysis of shaped nanoparticles synthesized using (A) monofunctional initiators (spherical particles), (B) mixed monofunctional and bifunctional initiators (spherical and dumbbell particles), and (C) mixed monofunctional and trifuctional initiators (spherical and tripartite particles). Histograms show the particle distributions (number of "joined" cores within each particle) resulting from each polymerization. (D) TEM image showing initiator directed tripartite nanostructures of different core sizes (all scale bars = 200 nm).

chains. This simple "effective functionality" rationale neither explains, however, the near absence of dumbbells in the case of initiator **8** nor explains the near-selective formation of triangular tripartite structures as opposed to, for example, linear "strings" of three conjoined cores. The preponderance of triangular shapes (Figure S17) could in principle be explained in terms of minimization of surface energy, but it is then surprising that triangular particles *and* linear/bent "strings" were observed in roughly equal proportions in the case of the bifunctional initiator (Figure S18).[15] Taken as a whole, these data suggest that the trifunctional initiator **8** may in fact direct the locus of the polymerization and the shape of the resulting polymer nanoparticle, even though these are "soft", flexible materials and each assembly is likely to contain significantly more than one trifunctional initiator.

Increasing the trifunctional/monofunctional initiator ratio, **8/1**, to 18:82 produced an insoluble, cross-linked gel. Hence, for the trifunctional initiator system, gelation occurs at a lower fraction of multifunctional initiator to monofunctional initiator compared to the bifunctional initiator where gelation occurred at a ratio of 25:75.[15] This is as expected when considering the role of average functionality in conventional gelation.

Conclusions

Branched amphiphilic block copolymers can be used to form well-defined organic nanoparticles by a one-pot direct synthesis, avoiding the need for postsynthesis self-assembly steps. We have shown that the mechanism of dumbbell formation is largely a concerted process of particle growth during polymerization, although it is probable that particle−particle linking also occurs, particularly at higher monomer conversions. Dumbbell particles formed using a cleavable initiator lead to cleavable dumbbells, underlining the degree of synthetic control and functionality placement that can be obtained even though the system is highly statistical and multicomponent in nature. The shape of branched polymer nanoparticles may be directed by the inclusion of multifunctional initiators, allowing the direct synthesis of "tripartite" nanoparticles which would be difficult to achieve through conventional synthesis/self-assembly/cross-linking strategies. Although the degree of shape control is imperfect, the formation of these structures with the limited selectively observed is nonetheless remarkable given the statistical nature of the chemistry and the "soft" nature of these polymers. Future work will focus on obtaining particles with higher structural purity by optimizing synthetic procedures and by exploiting size or mass separation techniques, for example, to obtain pure populations of asymmetric dumbbell particles with narrow size distributions.

Acknowledgment. The authors thank the Royal Society for an Industry Fellowship (S.R.) and acknowledge EPSRC (EP/C511794/1), Unilever, and the University of Liverpool for funding.

Supporting Information Available: Synthetic and experimental procedures, NMR spectra, GPC chromatograms, polymerization kinetics data, further TEM images, and DLS characterization. This material is available free of charge via the Internet at http://pubs.acs.org.

JA807462E